

Nonlinear Vibration Characteristics and Control of a Class of Piecewise Constrained Systems with Dynamic Gaps

Fei LIU*, Shuhui XU**, Zhuo TANG***, Qingzhen MA****

*Xi'an University of Science and Technology, Xian 710054, China,

**Xi'an University of Science and Technology Postdoctoral Research Station, Xian 710054, China,

*Xi'an Key Laboratory of Electrical Equipment Condition Monitoring and Power Supply Security, Xian 710054, China,

E-mail: liufei@xust.edu.cn

**Xi'an University of Science and Technology, Xian 710054, China, E-mail: xushuhui1996@126.com (Corresponding author)

***Xi'an University of Science and Technology, Xian 710054, China, E-mail: Tzzhuoo@163.com

****Xi'an University of Science and Technology, Xian 710054, China, E-mail: 20406050521@stu.xust.edu.cn

<https://doi.org/10.5755/j02.mech.33389>

1. Introduction

Due to elastic pre-tightening deformation, the collision between structures, mechanical assembly, and other factors that may make the system subject to Piecewise nonlinear constraint, piecewise nonlinear constraint generally exists in the mechanical system [1]. At the piecewise critical point, due to the sudden change of the constraint on the system, the motion trajectory at the piecewise is unpredictable, resulting in complex nonlinear vibration behavior of the system, which is not conducive to the stable operation of the system [2, 3].

In recent years, with the global attention to advanced science, the study of vibration characteristics of piecewise nonlinear systems has attracted widespread attention [4 – 6]. Liu considers the vibration instability caused by the assembly accuracy deviation of the roll nonlinear dynamic system with structural clearance in the hot rolling process. It is found that the instability of the system is a slowly changing process [7]. Yan considering that there may be clearance fit between the outer ring and the shell when the ball bearing works under complex conditions, the cage movement is seriously affected. A dynamic model of ball bearing with clearance fit is established to study the influence of clearance fit on cage movement. Some references are provided for the design and use of angular contact ball bearings [8]. Chen considering that the clearance seriously affects the motion accuracy and service life of the precision mechanism. The effects of clearance value, clearance shaft material and crank driving speed on the dynamic performance of the mechanism were studied. Finally, the correctness of the theoretical model is verified by experiment [9]. The Melnikov function of sub-harmonic orbit of piecewise system is studied in reference [10]. Shi considers a gap periodic forced vibration system composed of two-sided symmetric rigid constraints [11]. a establishes the dynamic model of the vibration impact system with non-fixed constraints. The results show that flutter is easy to occur in low frequency band, and viscous behavior occurs with the decrease of frequency ratio. Moreover, chattering is easy to occur with small clearance [12]. Amiri studied the dynamic behavior of the revolute joints of two planar mechanisms with gaps. By installing two vertical absorbers to control the clearance, the oscillation is significantly reduced. The results show that the designed vibrator has good robustness to

different parameters [13]. Tehrani considers Jeffcott rotors with rigid blades supported by oil film journal bearings. Two different gaps are analyzed separately. Due to the critical behavior of the system at low clearance values, the dual coupling of absorbers is used. The results show that the single coupling of the absorber can significantly reduce the vibration of the system. On the other hand, due to the low clearance value and low single coupling efficiency, dual coupling can be used to reduce the unnecessary vibration of the system [14]. Literature [15] proposed a modelless chaos control method based on AHGSA. Based on the idea of modelless adaptive control method, this method used the input/output data of the controlled system to estimate the pseudo-partial derivatives online, so as to establish a non-parametric time-varying dynamic linearization model of the system, and then de-signed a chaos controller based on the nonparametric time-varying dynamic linearization model. The parameters of the controller are optimized by AHGSA algorithm so that the chaotic motion is controlled as the expected periodic motion.

To sum up, although researchers have done a lot of research on the vibration mechanism of piecewise nonlinear systems and the control of system bifurcation behavior. However, the structure, material, wear, and other factors of the mechanical system will affect the piecewise nonlinear constraint of the system. The re-research on the influence of the change rate of piecewise nonlinear elastic force and the change of clearance on the stability of the system has not been further carried out. The research on bifurcation control of piecewise nonlinear system needs to be further improved. In this paper, we consider whether the change rate of piecewise nonlinear elastic force is inversely divided into two cases at the piecewise critical point, and study the influence of piecewise constraint on the stability of the system in two cases. and the influence of the number and clearance of different nonlinear constraints on the vibration characteristics of the system is analyzed. Finally, a sliding mode controller is designed to control the bifurcation behavior of the system.

2. The establishment of the model

2.1. Establishment of piecewise nonlinear constraint model

Although researchers observe the vibration behavior of the system from different angles, the piecewise nonlinear constrained system needs to be further studied.

Among them, the gear system is a typical piecewise nonlinear collision system, which has very complex non-smooth dynamic characteristics. It is well known that the gear system is the main transmission device of all kinds of mechanical equipment. The dynamic characteristics of gear system directly affect the working stability of mechanical equipment.

Assuming that the transmission shaft of the gear system is rigid and considering the torsional vibration of the support shaft, the vibration model of the single-degree-of-freedom driving wheel shown in Fig. 1 is established. The moment of inertia of the driving wheel is equivalent to fast mass m . The equivalent linear stiffness coefficient and equivalent linear damping of the driving wheel and the supporting plate are k_1 and c , respectively. F is the external disturbance force. x is the displacement of the mass block, and the right is defined as a positive direction.

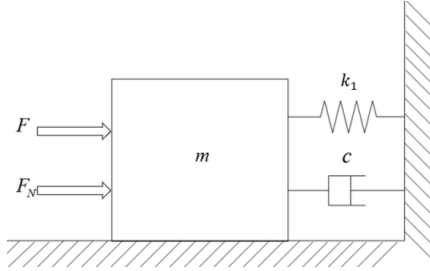


Fig. 1 Piecewise nonlinear constrained dynamic model

Because of the clearance between the gear teeth, the gear will be subjected to Piecewise nonlinear elastic force in the case of reciprocating torsion. Specifically, when the gear does not start the tooth engagement, the equivalent nonlinear stiffness of the mass block is k_2 , and when the displacement of the mass block is equal to e_2 , the nonlinear stiffness k_3 will act on the mass block, that is, the gear begins to tooth. After a period of time, the gearing begins to separate, and then the nonlinear stiffness of k_4 will occur when the displacement of the mass is equal to $-e_1$. Due to the different degree of wear on both sides of the gear and other factors, the size of e_1 and e_2 is different. Taking into account the general situation [16], the system is subject to Piecewise nonlinear elastic force as shown in the formula (1), and α is the cubic term coefficient:

$$F_N(x) = \begin{cases} -k_2 x & (e_2 < x) \\ -k_3 x & (-e_1 \leq x \leq e_2) \\ -k_4 x & (x < -e_1) \end{cases} \quad \begin{matrix} k_2 = (k_5 + \alpha k_6 x^2) \\ k_3 = (k_7 + \alpha k_8 x^2) \\ k_4 = (k_9 + \alpha k_{10} x^2) \end{matrix} \quad (1)$$

2.2. Establishment and solution of system dynamics model

Considering the piecewise nonlinear constraint, according to the generalized dissipative Lagrange principle, the dynamic equilibrium equation of the system subjected to periodic external disturbance force can be established as shown in formula (2):

$$m\ddot{x} + c\dot{x} + k_1 x - F_N(x) = F \sin(wt). \quad (2)$$

Dimensionless processing of the formula:

$$\ddot{x} = -c_1 \dot{x} - k_m x + F_n + F_m \sin(wt), \quad (3)$$

$$c_1 = \frac{c}{m}, k_m = \frac{k_1}{m}, F_n = \frac{F_N(x)}{m}, F_m = \frac{F}{m}.$$

The average method is used to solve the dynamic equation. Let the solution of the system be $x = a \cos(\phi)$, which can be obtained by bringing it into the above equation.

$$-\dot{a} \sin(\phi) + a \dot{\theta} \cos(\phi) = \frac{f(x, \dot{x})}{w}, \quad (4)$$

$$f(x, \dot{x}) = aw^2 \cos(\phi) - c_1 \dot{x} - k_m x + F_n + F_m \sin(wt).$$

And then according to the average method:

$$\dot{a} = \frac{-1}{2\pi w} \int_0^{2\pi} (f(x, \dot{x}) \sin(\phi)) d\phi$$

$$\dot{\theta} = \frac{-1}{2\pi wa} \int_0^{2\pi} (f(x, \dot{x}) \cos(\phi)) d\phi$$

The integral is calculated and the results are as follows:

$$\dot{a} = \frac{-1}{2\pi w} \left(\frac{caw}{m} \pi + \frac{F \pi \cos(\theta)}{m} + R_1 \right), \quad (5)$$

$$\dot{\theta} = \frac{1}{2\pi wa} \left(aw^2 \pi - \frac{k_1}{m} a \pi + \frac{2F \pi \sin(\theta)}{m} + R_2 \right). \quad (6)$$

$$\text{Among them, } R_1 = 0, R_2 = \int_0^{2\pi} (F_n \cos(\phi)) d\phi.$$

Through Eqs. (5) and (6), when $\dot{a} = 0$ and $\dot{\theta} = 0$, θ is eliminated. Finally, the relationship between the amplitude of the system and the frequency of the external disturbance force is as follows:

$$\left(\frac{caw}{F} \right)^2 + \left(\frac{\frac{k_1 a \pi}{m} - aw^2 \pi - R_2}{2F \pi} \right)^2 = 0. \quad (7)$$

3. Simulation research

In the establishment of the system model and the solution of the analytical solution, the system dynamics equation is solved numerically by the Runge-Kutta method. The effects of piecewise nonlinear constraint parameters and gaps on the amplitude-frequency characteristics, time-domain characteristics, bifurcation characteristics, and spectral characteristics of the system are studied.

3.1. The influence of the change rate of Piecewise nonlinear elastic force on the system

The sudden change of constraint in the system leads to complex and rich nonlinear phenomena such as bifurcation, chaos, and periodic coexistence in the dynamic response of the system. The dynamic behavior at the piecewise critical point will be more complex and more important. To study the influence of the piecewise constraint,

change rate on the system, it is divided into two cases according to whether the direction of the piecewise critical change rate changes or not. In case I, under the constraint, the values of the parameters are: $k_5=0.6$; $k_6=4.9$; $k_7=0.02$; $k_8=15$; $k_9=0.58$; $k_{10}=5$.

Under the constraint of case 2, the values of the parameters are as follow: $k_5=0.6$; $k_6=4$; $k_7=0.02$; $k_8=1$; $k_9=0.58$; $k_{10}=4.5$. Among them $e_1=4$; $e_2=3$; $c=0.12$; $m=1$; $k_1=1$ can be seen in Fig. 2, both of these two kinds of constraint will have a sudden change at the piecewise critical point, but the direction of the rate of change of the piecewise nonlinear elastic force at the piecewise critical point will not change with the change of displacement, the elastic force of case II changes in the direction of the rate of change of the Piecewise nonlinear elastic force at the piecewise critical point with the change of displacement.

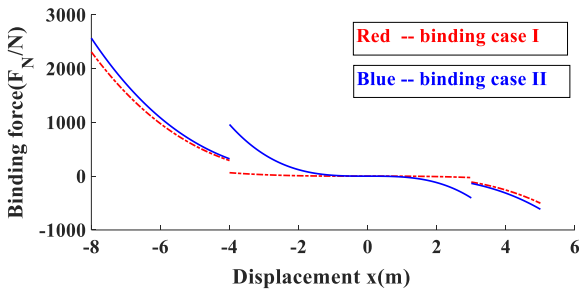


Fig. 2 Piecewise nonlinear restraint

Literature [17] also studied the dynamic characteristics of the nonlinear system, and the system received piecewise elastic forces, as shown in Fig. 3. Considering that the piecewise elastic force is continuous, the elastic force does not change abruptly at the piecewise critical point. However, in the actual mechanical system, there is a possibility of abrupt change of the piecewise elastic force at the piecewise critical point. Therefore, the elastic force model in this paper can more accurately analyze the dynamic behavior of the piecewise system at the piecewise critical point.

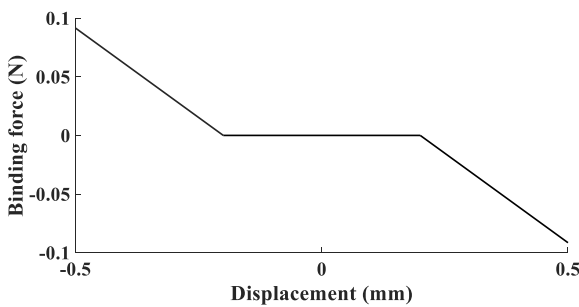


Fig. 3 The piece length elastic force of the system in reference [17]

To study the vibration of the system at the piecewise critical point under the influence of different constraint, the velocity curve of the simulation system is shown in Figs. 4 and 5. It is known that under the action of the constraint of case II vibration velocity of the mass vibration to the piecewise critical point fluctuates to a certain extent, which will aggravate the wear of the mechanical structure and reduce the reliability of the system. While the case I constraint acts, the system has almost no fluctuation in the vibration velocity of the system at the passing piecewise criticality, so it can be seen that the reverse change rate of

Piecewise nonlinear elastic force will greatly reduce the stability of the system at the piecewise critical point, which is not conducive to the normal operation of the system, which makes the vibration behavior of the unstable piecewise nonlinear system abnormal.

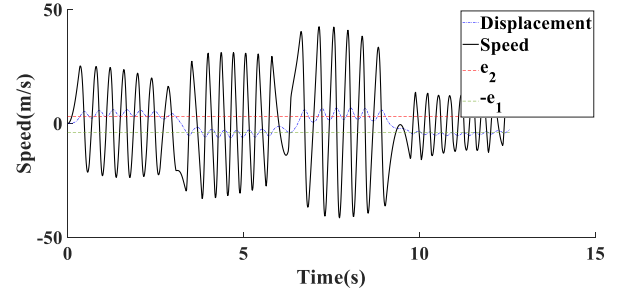


Fig. 4 Time domain curve under constraint case I

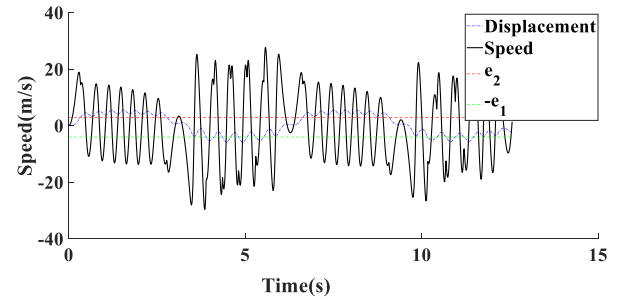


Fig. 5 Time domain curve under constraint force in case II

To better study the influence of Piecewise nonlinear elastic force on the system under two cases, the simulation study is carried out through its amplitude-frequency characteristic curve. It can be seen from Fig. 6 that under the action of the case II, there is a vibration amplitude jump phenomenon in the amplitude-frequency characteristic curve at the sectional critical point, which may lead to the fluctuation of the vibration amplitude of the system in the actual working conditions, resulting in abnormal vibration behavior. Under the action of the case I constraint, the jump phenomenon of the amplitude-frequency characteristic curve disappears at the piecewise critical point, and only a slight bending phenomenon will occur. Compared with the case II constraint, the system is more stable under the case I constraint.

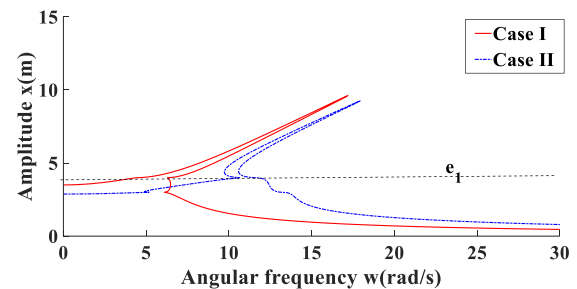


Fig. 6 Amplitude frequency curve under two constraint cases

Fig. 7 shows the amplitude-frequency characteristic curve of the system in literature [17]. At the critical point of the system piecewise, only slight bending occurs in the amplitude-frequency characteristic curve of the system, and no abrupt amplitude change occurs. Literature [17] did not take into account the law of the influence of the abrupt change of piecewise-elastic force on the system. Therefore, it is meaningful to consider the effect of sudden change of

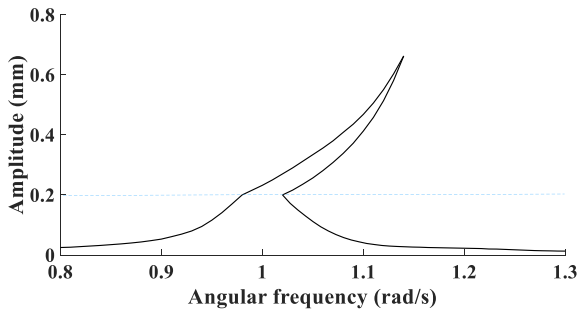


Fig. 7 Amplitude frequency curve under two constraint cases

elastic force and rate of change on vibration characteristics.

Fig. 8 shows that under the action of the case II constraint, the rate of change of the constraint is suddenly reversed at the piecewise critical position, which leads to the splicing of different phase trajectories before and after the critical point of the piecewise point, which indicates that the vibration behavior of the system has changed drastically, seriously affecting the normal operation of the mechanical system. However, under the action of case I constraint, the phase diagram is relatively smooth in the piecewise critical position, which can reduce the occurrence of system accidents.

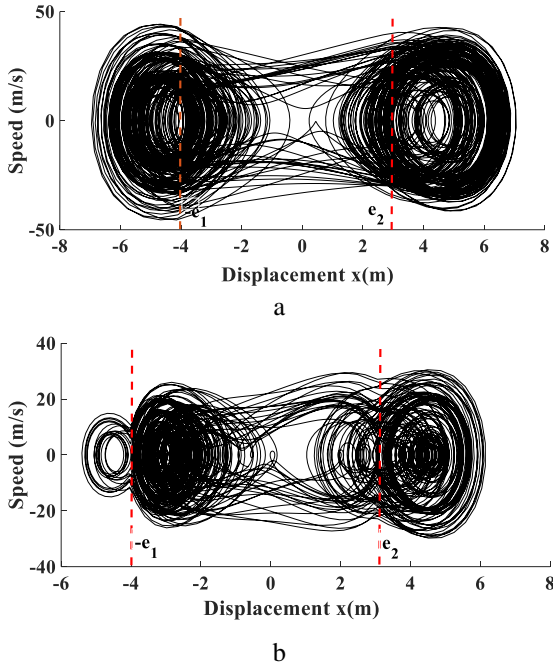


Fig. 8 Phase diagram under two constraint cases: a) case I; b) case II

In order to study the influence of nonlinear coefficients in piecewise nonlinear constraints on the system, the cubic coefficients α of piecewise nonlinear constraints are 0.2 and 2, respectively. As can be seen from Fig. 9, when piecewise nonlinear constraints increase, the amplitude-frequency curve of the system will deflect to the right more obviously, and the natural frequency of the system will increase. By controlling the cubic coefficient, the natural frequency of the system can be far away from the external disturbing force frequency and the occurrence of resonance can be reduced. With the increase of α , the frequency region of the external disturbance force increases at the critical point, which is not conducive to the stability of the system.

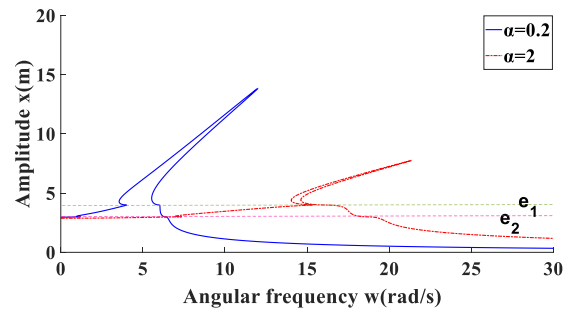


Fig. 9 α influence on amplitude frequency curve

Through the study, the change of the direction of the Piecewise nonlinear elastic force change rate will be not conducive to the stability of the system. In the actual working conditions, it is necessary to avoid this kind of constraint on the system as far as possible, so the piecewise nonlinear binding parameters are obtained as follows, which should be satisfied as much as possible in the actual working conditions to improve the stability of the system.

$$\begin{cases} (k_9 + k_{10}e_1^2) > (k_7 + k_8e_1^2) \\ (k_7 + k_8e_2^2) < (k_5 + k_6e_2^2) \end{cases} \quad (8)$$

3.2. The influence of the number of piecewise nonlinear constraints on the system

In the actual working conditions, the amplitude of the external disturbance force of the system is uncertain, which leads to the dynamic fluctuation of the vibration amplitude, so that the constraint of the system varies with the magnitude of the vibration displacement. furthermore, the system shows different dynamic characteristics under different constraints. When the vibration amplitude is less than e_1 , the system is subject to only one nonlinear constraint, when the vibration amplitude is greater than e_1 and less than e_2 , the system is subject to two-stage nonlinear constraints, and when the vibration amplitude is greater than e_2 , the system is subject to three-stage nonlinear constraints. The vibration characteristics of the system under three kinds of nonlinear constraints are analyzed by simulating vibration displacement, spectrum characteristics, and time-frequency characteristics.

From the displacement curve of Fig. 10, we can see that with the increase in the number of piecewise cases of constraints on the system, the system gradually diverges from approximate regular motion to chaotic motion, which proves that the more constrained the system is, the more unstable its motion is. According to the spectrum characteristic curve, with the increase in the number of cases subject to nonlinear constraints, the frequency components of the system become more and more complex. when subjected to three-stage nonlinear constraints, the frequency components of the system are disorganized and the influence of harmonic frequency increases. Under this constraint, it is difficult for the system to maintain a stable operation state.

According to the time-frequency curve of Fig. 11, when the system is subject to a period of binding constraints, its frequency component is relatively stable with the increase of time, and with the increase of the number of nonlinear constraints, the change of the frequency component of the system will become more and more violent, which

greatly increases the vibration frequency range of the system, resulting in the resonance behavior of the system more easily affected by external disturbance forces. Therefore, the

increase in the number of nonlinear constraints will gradually destroy the stability of the system, and it should be possible to reduce the number of nonlinear constraints on the system.

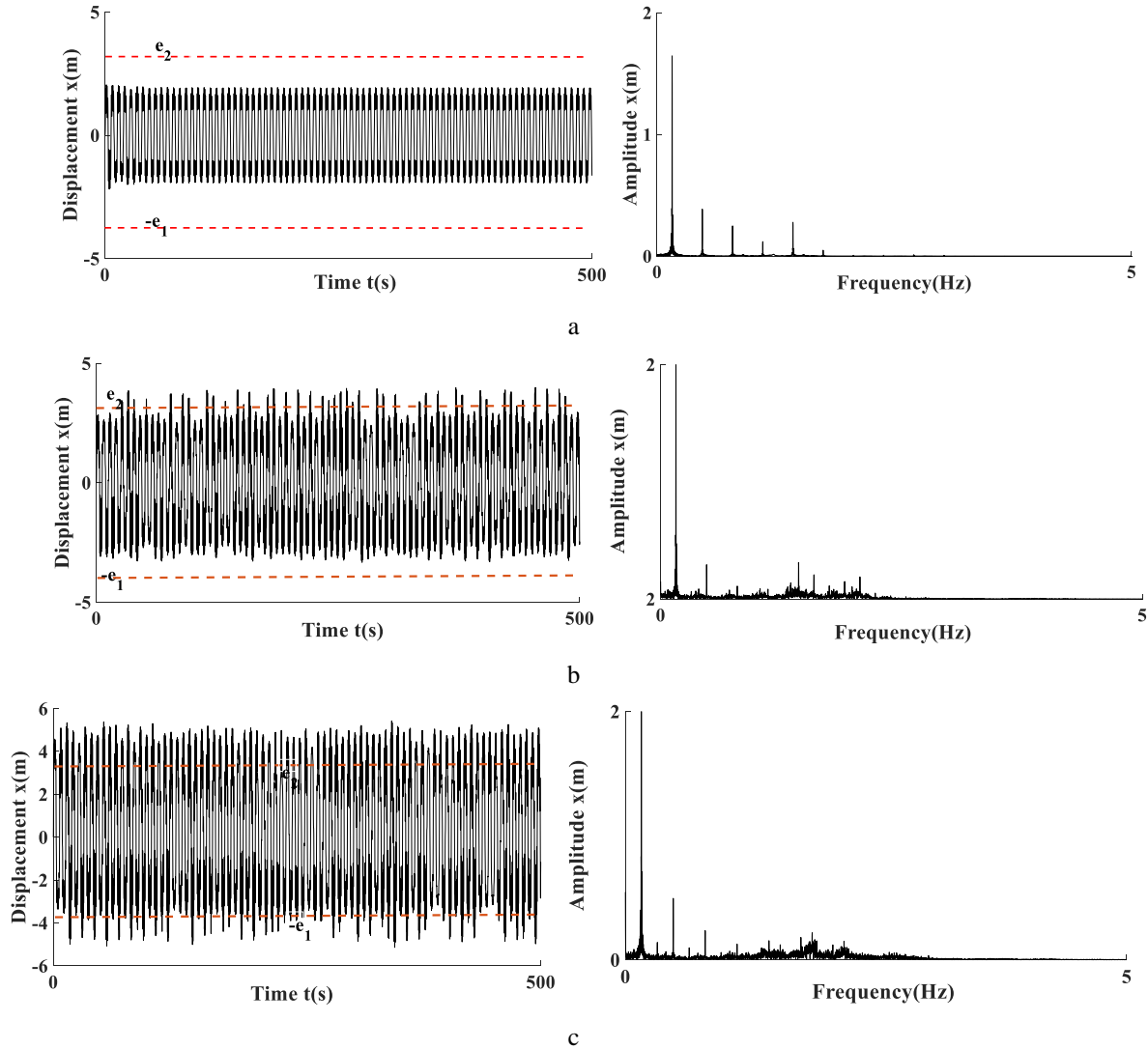


Fig. 10 Influence of the number of piecewise constraint cases on vibration characteristics: a) a constraint case; b) two-stage constraint case; c) three-stage constraint case

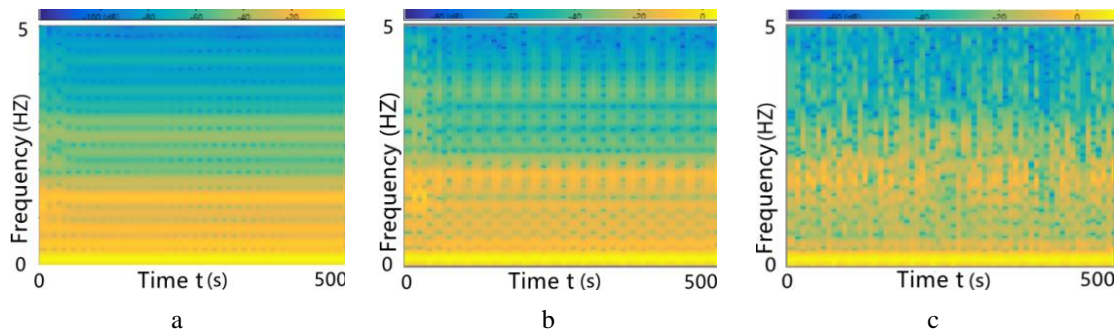


Fig. 11 Time frequency characteristics under three cases: a) a constraint case; b) two-stage constraint case; c) three-stage constraint case

3.3. Effect of clearance on the vibration behavior of the system

Mechanical structure wear, assembly and material aging lead to the change of initial pretension deformation and other factors, which will make the gap size change statically. In addition, in the actual working conditions, due to

the instability of the output force of the hydraulic system, the wear and relaxation of the mechanical structure and other reasons, all of them may lead to a dynamic change in the gap size of the piecewise constraint with time. To study the influence of clearance on the dynamic behavior of the system, the following simulation is carried out.

You can see from Fig. 12, with the decrease of e_1 , the

frequency interval of the multi-solution external disturbance force increases, and the vibration behavior of the system becomes complex and uncertain. Therefore, in the general mechanical structure should try to avoid the existence of too small clearance.

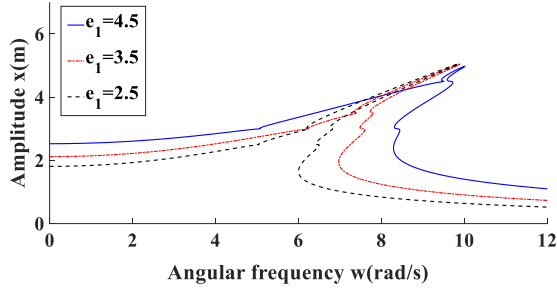


Fig. 12 e_1 Impact on amplitude frequency characteristics

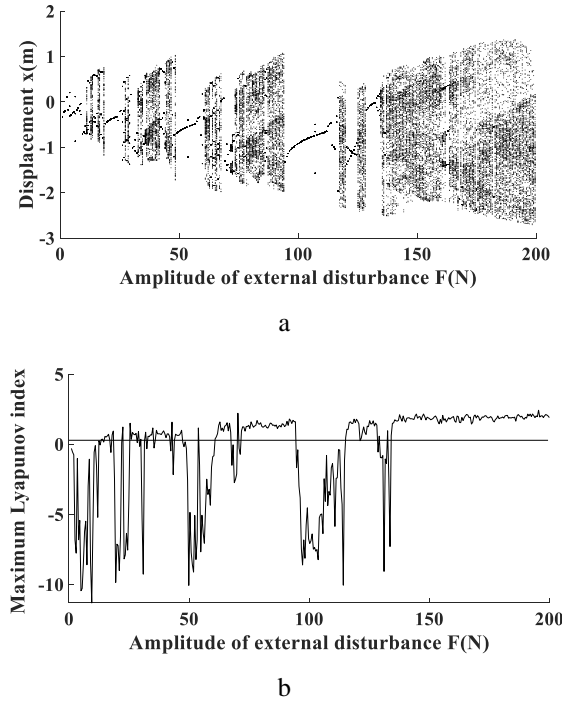


Fig. 13 Bifurcation characteristics with external disturbing forces: a) bifurcation diagram; b) maximum Lyapunov index

Fig. 13 shows the bifurcation characteristics of the system as the external disturbance force increases when $e_1=4$ and $e_2=3$. It can be seen that the system moves periodically when the external disturbance force is very small. With the increase of the external disturbance force, the vibration behavior of the system gradually diverges from periodic motion to chaotic motion, and the periodic motion and chaotic motion change alternately. When the system does periodic motion and period-doubling motion, the corresponding maximum Lyapunov exponent is less than or equal to 0, and when the system is in chaotic motion, the corresponding maximum Lyapunov exponent is less than 0. Combined with Fig. 14, we can see that when the external disturbance force is 131 N, the system moves periodically, the phase trajectory of the system is relatively simple, and the Poincare cross-section has only one point. When the amplitude of the external disturbance force is 133 N, the system does period-doubling motion, the phase trajectory of the system is more complex than the periodic motion, and the

Poincare cross-section shows two points. When the amplitude of the external disturbance force is 136 N, the system moves in chaos, the phase diagram trajectory of the system is complex, and the Poincare cross section shows many points. And with the increase of the amplitude of the external disturbance force, the vibration range of the displacement of the system in chaotic motion will also increase, so it can be seen that the excessive external disturbance force is not conducive to the stability of the system.

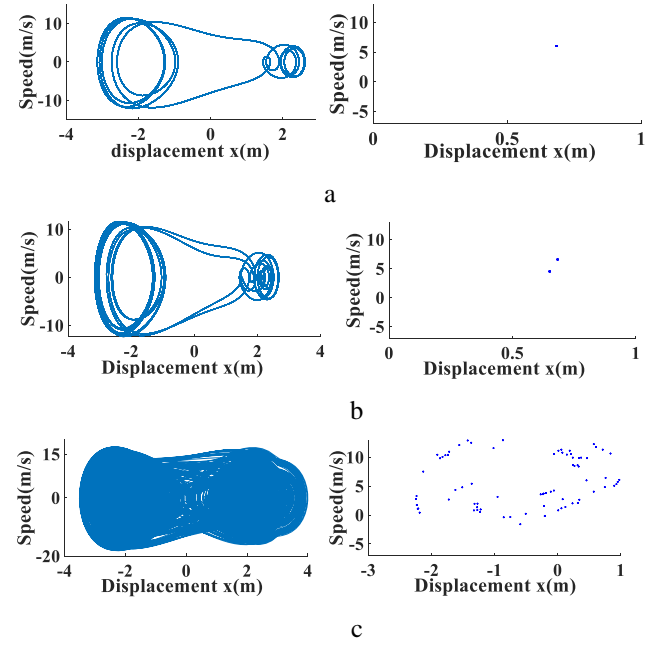


Fig. 14 Phase plane characteristics of the system under different amplitude of external disturbance force: a) $F=131$ N; b) $F=133$ N; c) $F=136$ N

To study the influence of the dynamic gap on the bifurcation characteristics of the system with time, it is considered that the wave momentum of the gap is $A \sin(w't)$. So, $e_1=4+A \sin(w't)$; $e_2=3+A \sin(w't)$, when $A=1.5$; $w'=10$, the bifurcation characteristics of the system vary with the external disturbance force are shown in Fig. 15. By comparison with Fig. 13, it can be seen that gap fluctuation will increase the frequency range of chaotic motion and the amplitude of displacement vibration will also increase. It can be seen that the dynamic fluctuation of the clearance will make the vibration behavior of the system in a more complex and unpredictable state.

In order to study the influence of gap fluctuation amplitude and frequency on the bifurcation characteristics of the system, the bifurcation characteristics of vibration displacement with the increase of fluctuation amplitude and frequency are simulated and analyzed, as shown in Figs. 16 and 17. It can be found that with the increase of clearance fluctuation amplitude and frequency, the motion state of the system gradually changes from periodic motion to chaotic motion, the vibration displacement interval gradually increases, and the stability of the system is gradually destroyed. Therefore, the above results show that the static gap size and dynamic gap fluctuation of the system are closely related to the stability of the system. The stability of the system will be seriously affected if the static clearance is too small and the fluctuation amplitude and frequency of the dynamic clearance are too large.

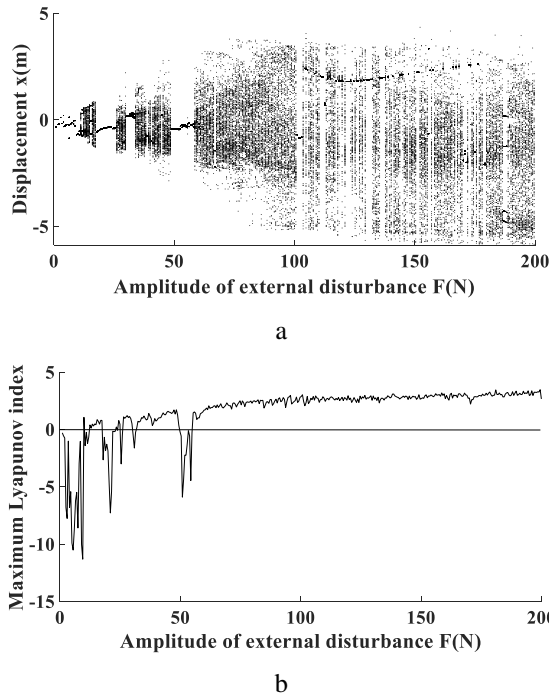


Fig. 15 Bifurcation characteristics with external disturbing forces: a) bifurcation diagram; b) maximum Lyapunov index

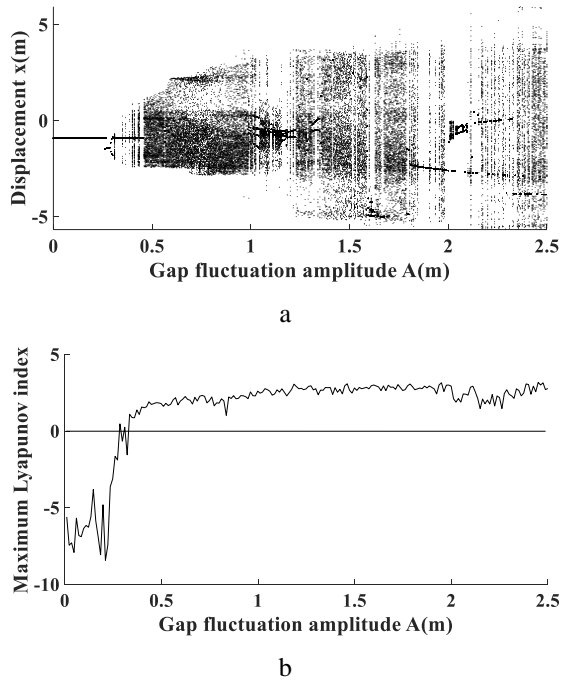


Fig. 16 Bifurcation characteristics with the variation of clearance fluctuation amplitude: a) bifurcation diagram; b) maximum Lyapunov index

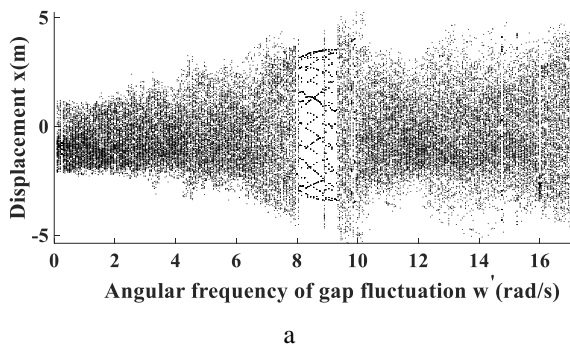


Fig. 17 Bifurcation diagram with clearance fluctuation frequency: a) bifurcation diagram; b) maximum Lyapunov index

4. Research on sliding mode bifurcation control

Because the sliding mode variable structure control can choose the corresponding control rate according to the current state of the system, the control for the piecewise system has great advantages [18]. However, because the control rate needs to be switched frequently, the sliding mode controller has the disadvantage of chattering. To make up for the deficiency of the controller, it is considered to restrain the chattering behavior of the system by adding differential control. Therefore, the combination of sliding mode control and Differential control is used to restrain the chaotic motion behavior of the system. Fig. 18 is the principle block diagram of sliding mode variable structure control.

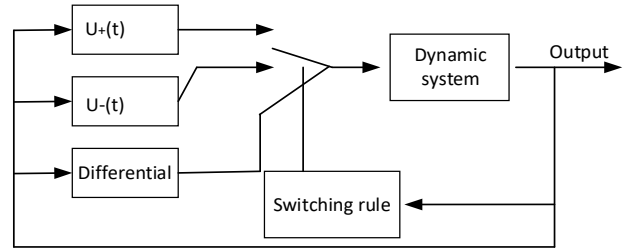


Fig. 18 Control schematic diagram

To facilitate the design of sliding mode controller, the piecewise nonlinear constraint is expressed by two functions:

$$F_n(x) = \begin{cases} F_n^+(x) & (x \geq 0) \\ F_n^-(x) & (x < 0) \end{cases}$$

$$F_n^+(x) = (k_2 + k_3 x^2) x M_1 + (k_4 + k_5 x^2) x M_2$$

$$F_n^-(x) = (k_4 + k_5 x^2) x M_3 + (k_6 + k_7 x^2) x M_4.$$

$$\text{Among them: } M_1 = \frac{1 + \text{sgn}(x - e_2)}{2},$$

$$M_2 = \frac{1 - \text{sgn}(x - e_2)}{2}, \quad M_3 = \frac{1 + \text{sgn}(x + e_1)}{2},$$

$$M_4 = \frac{1 - \text{sgn}(x + e_1)}{2}.$$

The dynamic equation of the system can be expressed as follows:

$$\ddot{x} = -c_1 \dot{x} - k_m x + F_K + F_m \sin(\omega t) + \tau u(x, t), \quad (9)$$

where: $u(x, t)$ is a sliding mode variable structure controller; τ is the controller gain coefficient; $F_K = F_n/m$.

First, a linear sliding surface is designed:

$s(t) = \delta x(t) + \dot{x}(t)$, $\delta > 0$. Selection index approach rate: $\dot{s} = -\gamma \text{sgn}(s(t)) - bs(t)$, $\gamma > 0, b > 0$.

The derivation of the above formula can be obtained: $\dot{s}(t) = \delta \dot{x}(t) + \ddot{x}(t)$. The sliding mode control rate can be obtained by combining the above formula, and the control rate of the Differential control can be expressed as $-\mu \dot{x}$. The control rate of the controller under the combined action of sliding mode control and differential control is:

$$u(t) = \begin{cases} u_+(t), & s(t) > 0 \\ u_-(t), & s(t) < 0 \end{cases}, \quad (10)$$

$$u_+(t) = -\delta \dot{x} - \gamma \text{sgn}(s(t)) - bs(t) - c_1 \dot{x} - k_m x + \frac{F_n^+(x)}{m} + F_m \sin(\omega t) - \mu \dot{x}; \quad u_-(t) = -\delta \dot{x} - \gamma \text{sgn}(s(t)) - bs(t) - c_1 \dot{x} - k_m x + F_n^-(x) / m + F_m \sin(\omega t) - \mu \dot{x}.$$

4.1 Time domain and frequency domain characteristics of the system under differential sliding mode control

The control effect of sliding mode control, differential control and differential sliding mode control is compared by time domain and frequency domain characteristics, the relevant parameters of the controller are as follows: $b=6$; $\gamma=6$; $\delta=1000$; $\tau=0.004$; $\mu=30$.

When the change of clearance is a , observe Fig. 19. It can be found that the vibration displacement of the system at this time is chaotic, and the vibration amplitude is large, the frequency component of the vibration is also very complex, and the probability of triggering resonance is high. Fig. 20 shows the displacement curve and spectrum diagram of the system vibration when the differential control is introduced. It can be found that the differential controller has an inhibitory effect on the vibration amplitude of the system, but the frequency component of the system hardly changes.

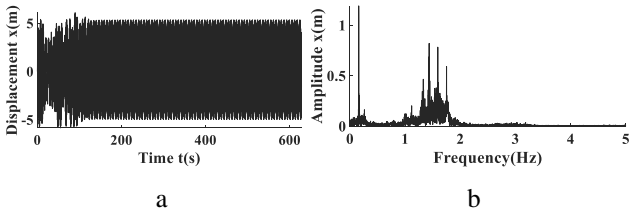


Fig. 19 Vibration characteristics of the system when no control is introduced: a) vibration displacement; b) spectral diagram

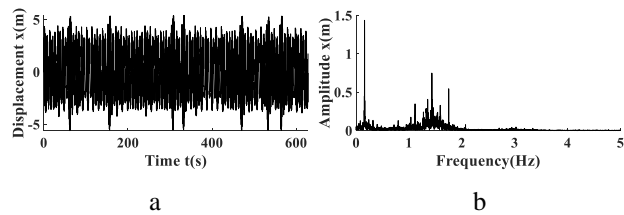


Fig. 20 Vibration characteristics of the system under the action of differential control: a) vibration displacement; b) spectral diagram

Fig. 21 shows the introduction of a sliding mode controller. The vibration displacement characteristics of the

system tend to be in a state of periodic motion, and its frequency components become more simple. However, the displacement curve still presents chattering with ups and downs, which is not conducive to the stability of the system. In order to eliminate chattering phenomenon, differential control and sliding mode control are added to the system at the same time. As shown in Fig. 22, chattering phenomenon of vibration displacement of the system disappears and the system is in a state of periodic motion. Therefore, the sliding mode variable structure controller combined with the differential control can effectively suppress the vibration amplitude of the system, reduce the frequency component of the system, and effectively improve the stability of the system.

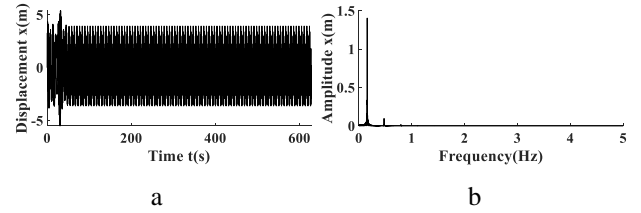


Fig. 21 Vibration characteristics of the system under sliding mode control: a) vibration displacement; b) spectral diagram

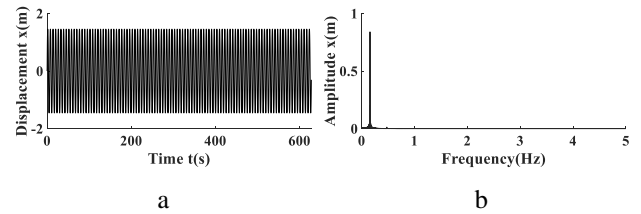


Fig. 22 Vibration characteristics of the system under differential sliding mode control: a) vibration displacement; b) spectral diagram

4.2. Bifurcation characteristics of the system under control

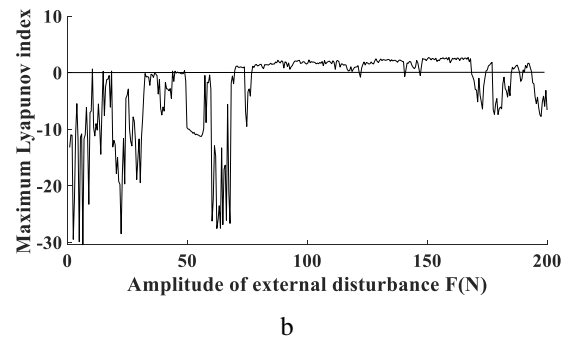
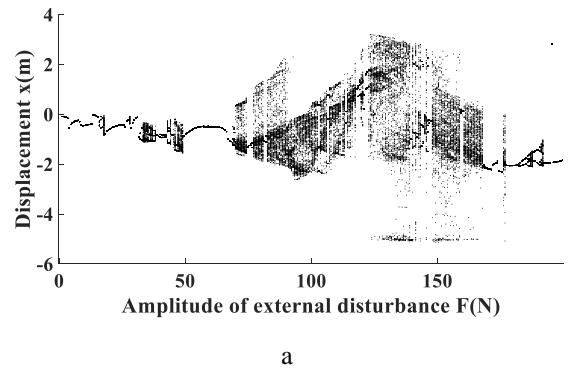


Fig. 23 Bifurcation characteristics with external disturbance force by introducing sliding mode controller: a) bifurcation diagram; b) maximum Lyapunov index

The effectiveness of the sliding mode controller is verified by the bifurcation characteristics, and the relevant parameters of the controller are as follows: $b=6$; $\gamma=6$; $\delta=1000$; $\tau=0.002$; $\mu=0.5$. Compared with Figs. 15 and 23, it is found that after the introduction of the differential sliding mode controller, the chaotic state of the system is suppressed with the increase of external disturbance force, and the chaotic motion state of the system will appear at about 20 N, which shows that the controller can effectively improve the stability of the system under external excitation.

By increasing the influence coefficient of the controller, as shown in Fig. 24, it can be found that the chaotic motion interval of the bifurcation characteristics of the system under the change of external disturbance force is further reduced, and it is periodic motion before the external disturbance force is 90 N. It can be seen that the controller can effectively control the chaotic motion of the system.

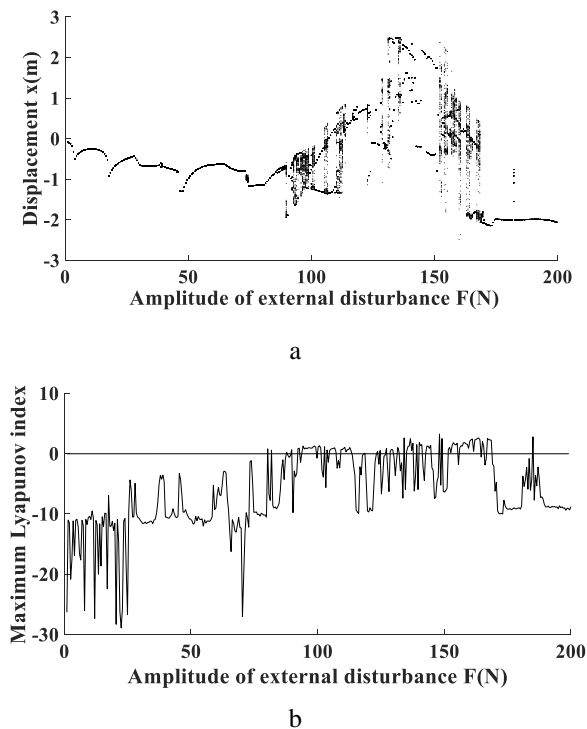


Fig. 24 Bifurcation characteristics with external disturbance force by introducing sliding mode controller: a) bifurcation diagram; b) maximum Lyapunov index

5. Conclusions

In this paper, the mass block system under piecewise nonlinear constraints is considered, and the vibration dynamic model is established according to the generalized dissipative Lagrange principle. The analytical and numerical solutions of the system are obtained by the averaging method and the Runge-Kutta method.

The influence of the change rate of piecewise nonlinear constraint on the motion state of the system at the piecewise critical point is analyzed using time domain characteristics, phase plane characteristics and amplitude-frequency characteristics, it is found that the reverse of the piecewise nonlinear constraint change rate will make the vibration velocity of the system fluctuate sharply, the phase trajectory changes obviously, and the amplitude jump phenomenon exists at the piecewise critical place, which is not conducive to the normal operation of the mechanical sys-

tem. Therefore, the reverse change rate of Piecewise nonlinear elastic force is avoided as far as possible, and the relationship between piecewise nonlinear constraint parameters is obtained, which provides a theoretical basis for improving the stability of the system.

The effect of the number of nonlinear constraints on the vibration characteristics of the system is studied. It is found that with the increase of the number of piecewise, the frequency component of the system becomes more complex, the displacement curve tends to be chaotic, and the time-frequency characteristics change more violently. Because of its susceptibility to resonance, the system should be subject to a single constraint as far as possible. The results show that the smaller the static clearance is, the larger the instability frequency interval is. The dynamic change of the gap will increase the frequency range of chaotic motion, expand the range of vibration displacement, and aggravate the unpredictable chaotic state of the system. With the increase of clearance fluctuation amplitude and frequency, the vibration behavior of mechanical system becomes complicated and unstable. It can be found that the static gap size, dynamic gap fluctuation amplitude and frequency are negatively correlated with the system stability.

A differential sliding mode controller is used to control the vibration characteristics of the system, and the effects of differential control, sliding mode control and differential sliding mode control on the vibration characteristics of the system are compared and analyzed. The results show that the introduction of differential sliding mode controller can effectively suppress the chaotic motion of piecewise constrained systems with dynamic gaps. It provides a theoretical reference for vibration behavior control of piecewise constrained systems with dynamic gaps.

Declaration of conflicting interests

The authors declare no conflict of interest in preparing this article.

Data availability statement

No data were used to support this study.

Acknowledgment

This work was funded by the National Natural Science Foundation of China (grant number 51905416), Scientific Research Program of Shaanxi Provincial Education Department (grant number 20JK0758).

References

1. Kurvinen, E.; Viitala, R.; Choudhury, T.; et al. 2020. Simulation of subcritical vibrations of a large flexible rotor with varying spherical roller bearing clearance and roundness profiles, *Machines* 8. <https://dx.doi.org/10.3390/machines8020028>.
2. Patra, P.; Saran, V. H.; Harsha, S. P. 2020. Vibration response analysis of high-speed cylindrical roller bearings using response surface method, *Proceedings of the Institution of Mechanical Engineers Part K-Journal of Multi-Body Dynamics* 234: 379-392. <https://dx.doi.org/10.1177/1464419320910864>.

3. **Fontanela, F.; Vizzaccaro, A.; Auvray, J.; et al.** 2021. Nonlinear vibration localisation in a symmetric system of two coupled beams, *Nonlinear Dynamics* 103: 3417-3428.
<https://dx.doi.org/10.1007/s11071-020-05760-x>.
4. **Liu, J.; Xue, L.; Ni, H.** 2022. Vibration simulation of the turbine rotor system of an underwater vehicle considering the bearing radial clearance, *International Journal of Acoustics and Vibration* 27: 393-401.
<https://dx.doi.org/10.20855/ijav.2022.27.41899>.
5. **Gao, X.; Niu, J.; He, L.; et al.** 2023. Vibration characteristics of multi-dimensional isolator based on 4-PUU parallel mechanism with joint clearance, *Nonlinear Dynamics* 111:5179-5195.
<https://dx.doi.org/10.1007/s11071-022-08117-8>.
6. **Soobbarayen, K.; Besset, S.; Sinou, J. J.** 2013. Noise and vibration for a self-excited mechanical system with friction, *Applied Acoustics* 74:1191-1204.
<https://dx.doi.org/10.1016/j.apacoust.2013.03.008>.
7. **Cui, J.; Peng, Y.; Wang, J.** 2023. Instability of roll nonlinear system with structural clearance in rolling process, *Journal of Iron and Steel Research International* 30:112-125.
<https://dx.doi.org/10.1007/s42243-022-00816-1>.
8. **Yan, S.; Qu, Q.; Liu, M.** 2023. Investigation on cage motions in high speed angular contact ball bearing with clearance fit between the outer ring and housing, *Proceedings of The Institution of Mechanical Engineers Part K-Journal of Multi-Body Dynamics* 237: 86-97.
<https://dx.doi.org/10.1177/14644193221129648>.
9. **Chen, X.; Gao, S.; Wang, T.; et al.** 2022. Experimental verification of dynamic behavior for multi-link press mechanism with 2D revolute joint considering dry friction clearances and lubricated clearances, *Nonlinear Dynamics* 109:707-729.
<https://dx.doi.org/10.1007/s11071-022-07478-4>.
10. **Li, S.; Zhao, S.** 2019. The analytical method of studying subharmonic periodic orbits for planar piecewise-smooth systems with two switching manifolds, *International Journal of Dynamics and Control* 7: 23-35.
<https://dx.doi.org/10.1007/s40435-018-0433-z>.
11. **Shi, Y.** 2019. Periodic vibration and bifurcation of vibratory systems with clearance composed of rigid constraints, *Materials Science and Engineering* 612: 032058.
<https://dx.doi.org/10.1103/PhysRevLett.51.623>.
12. **Du, Y.; Zhang, G.** 2019. Research on chattering occurrence condition in a vibro-impact system, *Journal of Low Frequency Noise Vibration and Active Control* 38: 1202-1213.
<https://dx.doi.org/10.1177/1461348418813289>.
13. **Amiri, A.; Dardel, M.; Daniali, H. M.** 2019. Effects of passive vibration absorbers on the mechanisms having clearance joints, *Multibody System Dynamics* 47: 363-395.
<https://dx.doi.org/10.1007/s11044-019-09684-2>.
14. **Tehrani, G. G.; Dardel, M.; Pashaei, M. H.** 2020. Passive vibration absorbers for vibration reduction in the multi-bladed rotor with rotor and stator contact, *Acta Mechanica* 231: 597-623.
<https://dx.doi.org/10.1007/s00707-019-02557-x>.
15. **Wei, X.; Li, N.; Ding, W.; et al.** 2018. Model-free chaos control based on AHGSA for a vibro-impact system, *Nonlinear Dynamics* 24: 1-11.
<https://dx.doi.org/10.1007/s11071-018-4397-5>.
16. **Liu, Z.; Li, P.; Jiang J.; et al.** 2021. Research on vibration characteristics of mill rolls based on nonlinear stiffness of the hydraulic cylinder, *Journal of Manufacturing Processes* 64: 1322-1328.
<https://dx.doi.org/10.1016/j.jmapro.2021.02.063>.
17. **Sun, Y.** 2021. Experimental modelling and amplitude-frequency response analysis of a piecewise linear vibration system, *IEEE Access* 9: 4279-4290.
<https://dx.doi.org/10.1109/ACCESS.2020.3047655>.
18. **Paul, S.; Yu, W.; Li, X. O.** 2019. Discrete-time sliding mode for building structure bidirectional active vibration control, *Transactions of the Institute of Measurement and Control* 41: 433-446.
<https://dx.doi.org/10.1177/0142331218764581>.

F. Liu, S. Xu, Z. Tang, Q. Ma

NONLINEAR VIBRATION CHARACTERISTICS AND CONTROL OF A CLASS OF PIECEWISE CONSTRAINED SYSTEMS WITH DYNAMIC GAPS

S u m m a r y

Considering the mass block system under Piecewise nonlinear constraint, the vibration dynamic model of the system is established according to the generalized dissipative Lagrange principle, and the average method is used to solve the amplitude-frequency response of the vibration system. The influence of system parameters on vibration characteristics is analyzed with amplitude-frequency characteristics, phase plane characteristics, frequency characteristics, bifurcation characteristics, and so on. The results show that: 1) the reverse of the rate of change of Piecewise nonlinear elastic force will destroy the stability of the system and obtain the relationship of the constraint parameters that need to be satisfied when the system is stable at the piecewise critical point; 2) With the increase in the number of nonlinear constraints, the vibration displacement of the system tends to be chaotic, and the frequency composition becomes more complex and variable, prone to resonance behavior; 3) As the static gap decreases and the dynamic gap amplitude and frequency increase, the unstable frequency range of the system will increase, and the vibration behavior will become chaotic and difficult to predict; 4) The design of a differential sliding mode controller can effectively control the bifurcation behavior of the system.

Keywords: piecewise nonlinear constraints, dynamic clearances, bifurcation characteristics, sliding mode control.

Received February 11, 2023

Accepted October 9, 2023



This article is an Open Access article distributed under the terms and conditions of the Creative Commons Attribution 4.0 (CC BY 4.0) License (<http://creativecommons.org/licenses/by/4.0/>).